INTERNATIONAL JOURNAL FOR NUMERICAL METHODS IN FLUIDS
Int. J. Numer. Meth. Fluids **29**: 625–644 (1999)

STUDY OF THE EFFECT OF THE NON-ORTHOGONALITY FOR NON-STAGGERED GRIDS—THE RESULTS

HAO XU* AND C. ZHANG

Department of Mechanical and Materials Engineering, University of Windsor, Windsor, Ontario N9B 3P4, Canada

SUMMARY

This article presents the effect of the grid skewness on the ranges of the underrelaxation factors for pressure and velocity. The effect is reflected by the relationship between the numbers of iterations required and the ranges of the underrelaxation factors for a converged solution. Four typical cavity flow problems are solved on non-staggered grids for this purpose. Two momentum interpolation practices namely, practice A and practice B, together with SIMPLE, SIMPLEC and SIMPLER algorithms are employed. The results show that the ranges of the pressure underrelaxation factor values for convergence exist if the SIMPLE algorithm is used, while no restrictions are observed if the SIMPLEC algorithm is used. From the curves obtained using the SIMPLER algorithm, the ranges of those based on practice B are wider than those based on practice A. Copyright © 1999 John Wiley & Sons, Ltd.

KEY WORDS: lid-driven cavity flow; non-staggered grid; momentum interpolation; underrelaxation factor

1. INTRODUCTION

In a companion article [1], the contravariant velocity fluxes were chosen as the dependent variables on the non-staggered, non-orthogonal grids. The discretization equations for the Navier–Stokes equations in general curvilinear co-ordinates retain a strongly conservative form. The momentum interpolation was introduced to avoid the splitting of the pressure field. In order to carry out the momentum interpolation, two different practices, namely, practice A and practice B, were presented to calculate the values of the contravariant velocity fluxes at the faces of the control volumes. In each practice, two cases of the momentum interpolation formulations, with and without the velocity underrelaxation factor, are considered. The SIMPLE [2], SIMPLER [3] and SIMPLEC [4] algorithms were employed to solve the governing equations. Each of these three algorithms was combined with each of the cases in each practice. The purpose of this work is to study the effect of the grid non-orthogonality on the ranges of the underrelaxation factors. These ranges are indicated on the plots of the numbers of the iterations required for convergence versus the ranges of the underrelaxation factors. The typical two-dimensional lid-driven cavity flows as shown in Figure 1 are selected for this purpose. In the present study, the non-orthogonal terms in the pressure-correction equation are omitted.

* Correspondence to: Department of Mechanical and Materials Engineering, University of Windsor, Windsor, Ontario N9B 3P4, Canada.

CCC 0271–2091/99/060625–20$17.50

Received February 1997
Revised May 1997

Previously, Peric [5] studied the effect of the grid non-orthogonality on the convergence behavior for the two-dimensional lid-driven cavity flows with $\beta = 90$, 60, 45 and 30° respectively. Peric compared the results obtained from the simplified pressure-correction equation (the non-orthogonal terms are neglected), in which five nodes for 2D flows and seven nodes for 3D flows are used in the coefficient matrix, with those obtained from the full one, in which nine nodes for 2D flows and 19 nodes for 3D flows are used in the coefficient matrix. Peric found that it is more efficient to use the simplified pressure-correction equation than its full form if the grids are not severely non-orthogonal, and it is necessary to use the full pressure-correction equation if the grids are significantly non-orthogonal. The simplified version either does not give a converged solution at all or the convergence is too slow if the grids are severely non-orthogonal. For a given velocity underrelaxation factor, the range of the pressure underrelaxation factor that can be used for a converged solution becomes narrower, as the skewness of the non-orthogonal grid increases if the simplified pressure-correction equation is employed. However, this phenomenon does not occur if one uses the full pressure-correction equation. For a given skewness of the grid, the range of the pressure underrelaxation factor for a converged solution gets narrower as the velocity underrelaxation factor increases. This applies to both results obtained using the simplified and the full pressure-correction equations. But the range of the pressure underrelaxation factor gets narrow much faster if the simplified pressure-correction equation is used than that if the full one is used. Recently, Cho and Chung [6] proposed a new treatment method for non-orthogonal terms in the pressure-correction equation in order to enlarge the ranges of the values of the pressure underrelaxation factor for convergence. In this new treatment, the non-orthogonal terms in the full pressure-correction equation are decomposed into explicit and implicit terms and five nodes for 2D flows and seven nodes for 3D flows are used in the coefficient matrix for the pressure-correction equation. Although this treatment is superior to the simplified treatment if the grids are significantly non-orthogonal, its pressure-correction equation is more complex than the simplified one. In both studies [5,6], the SIMPLE algorithm was used to solve the governing equations on 20×20 control volumes or grids with $Re = 100$. The analyses in [5,6], in the investigators' words, are valid for both staggered and non-staggered grid arrangements.

In the present research, four cases of the cavity flows are studied, namely, $\beta = 90$, 60, 45 and 30°. Reynolds number based on the definition of $(\rho u_L L/\mu)$ is set to be 100 in all cases. The calculation is carried out on the uniform 20×20 grids. The convergence is thought to be

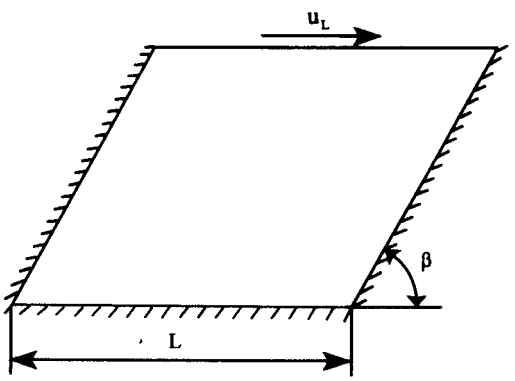

Figure 1. Geometry of the lid-driven cavity flow.

achieved when the sum of the absolute values of the residuals in all the equations is less than 10^{-4}. In this article, some new discoveries regarding the effect of the grid non-orthogonality for the lid-driven cavity flows are presented. First, the results using the SIMPLE algorithm are shown for four cases of the cavity flows using the two momentum interpolation practices with and without α_{U^i}. To the best of the authors' knowledge, there are no reports on the study of the relationship between the numbers of iterations and the ranges of the underrelaxation factors using the SIMPLEC and SIMPLER algorithms. Next, the results using these two algorithms are given. Equations (41) and (43) and Equations (44) and (45) in the companion article [1] are referred to as the two momentum interpolation practices with and without the velocity underrelaxation factor, α_{U^i} respectively. Some concomitant explanations regarding α_{U^i} can also be found in [1].

2. RESULTS OF CALCULATIONS

Figures 2–45 show the convergence properties for the cavity flows. It is noted here that the legends used in Figures 3–45 are the same as those in Figure 2.

Figures 2–21 show the numbers of iterations required for convergence by using the SIMPLE algorithm [2] as a function of the pressure underrelaxation factor, α_p, with the velocity underrelaxation factor, α_{U^i}, as a parameter. Figures 2–6 are for $\beta = 90°$, Figures 7–11 for $\beta = 60°$, Figures 12–16 for $\beta = 45°$, while Figures 17–21 for $\beta = 30°$.

First of all, the convergence can always be reached for both practices, but very slowly if α_{U^i} is very small. Study of the behavior of the grid non-orthogonality for $\alpha_{U^i} < 0.5$ is not necessary and valuable because α_p can reach 1.0 for both practices if $\alpha_{U^i} < 0.5$. Also, the use of very small values for α_{U^i} is not practical since the convergence is too slow. On the other hand, using $\alpha_{U^i} = 1.0$ results in a diverged solution for both practices. In the present study, α_{U^i} value is set to be 0.5, 0.6, 0.7, 0.8 and 0.9 as a parameter, and $\alpha_p = 0.1$ is chosen as the starting point for each curve. For practice A, the convergence cannot be obtained for $\alpha_{U^i} = 0.9$ in all four cases of the cavity flows. Therefore, the convergence behaviors are not plotted in the corresponding figures for this practice when $\alpha_{U^i} = 0.9$. Practice B does not have this difficulty. For practice A without α_{U^i} and practice B with and without α_{U^i}, α_p can reach 1.0 for $\alpha_{U^i} \leq 0.6$ when $\beta = 90$, 60 and 45°, and for $\alpha_{U^i} \leq 0.5$ when $\beta = 30°$. The α_{U^i} value for obtaining a full range of α_p value decreases as the skewness of the non-orthogonal grid gets higher (β decreases). For practice A with α_{U^i}, such α_{U^i} values are lower than those for practice A without α_{U^i}, and practice B with and without α_{U^i}.

As it has been expected, the convergence rate depends strongly on the underrelaxation factors α_p and α_{U^i}, and the grid skewness, which is reflected by the angle β. If α_{U^i} value is given, the range of α_p values becomes narrower as the grid skewness gets higher. This phenomenon is not obvious for the results based on practice A, but can be seen clearly from the results based on practice B. If the grid skewness is fixed (β is fixed), the range of α_p values becomes narrower as α_{U^i} increases. The number of iterations required for convergence decreases as the grid skewness decreases. This is especially obvious for small α_p values. On each curve, there is an optimum α_p value for getting a least number of iterations required for convergence, this value may not be 1.0. It is 1.0 when a full range of α_p values exists, except for practice A with α_{U^i}. It is obvious that the range of α_p values obtained using practice B is wider than that obtained using practice A. In practice A, this range based on the case of without α_{U^i} is wider than that based on the case of with α_{U^i}. There is almost no difference between the two cases for practice B.

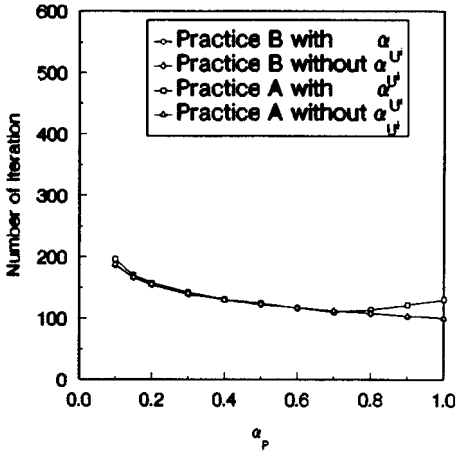

Figure 2. Convergence properties for SIMPLE: $\beta = 90°$, $\alpha_{Ui} = 0.5$.

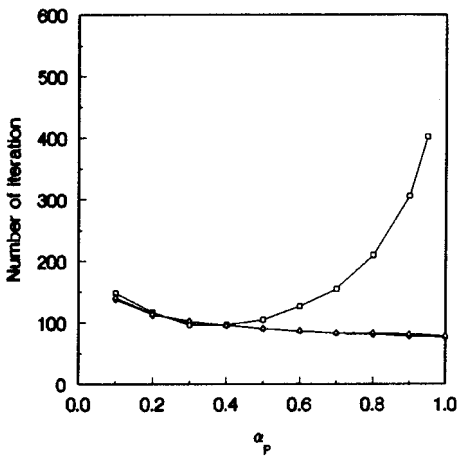

Figure 3. Convergence properties for SIMPLE: $\beta = 90°$, $\alpha_{Ui} = 0.6$.

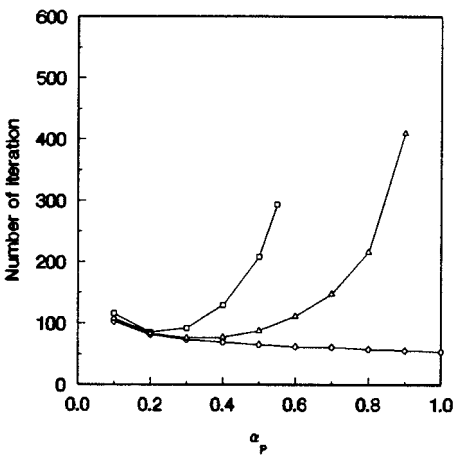

Figure 4. Convergence properties for SIMPLE: $\beta = 90°$, $\alpha_{Ui} = 0.7$.

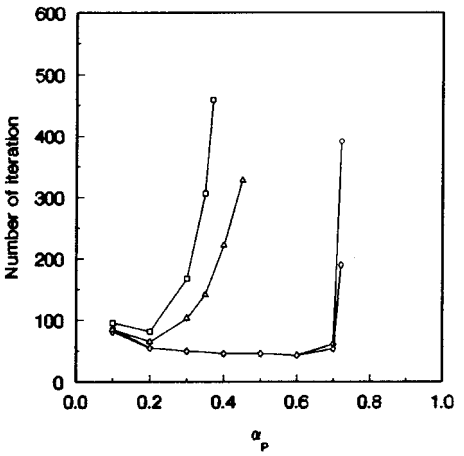

Figure 5. Convergence properties for SIMPLE: $\beta = 90°$, $\alpha_{Ui} = 0.8$.

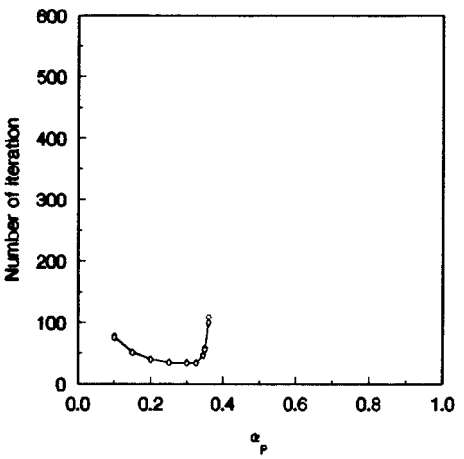

Figure 6. Convergence properties for SIMPLE: $\beta = 90°$, $\alpha_{Ui} = 0.9$.

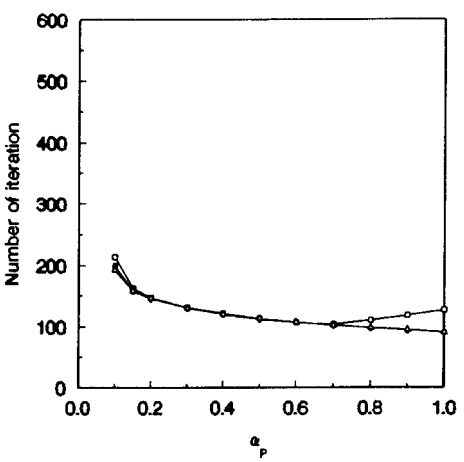

Figure 7. Convergence properties for SIMPLE: $\beta = 60°$, $\alpha_{Ui} = 0.5$.

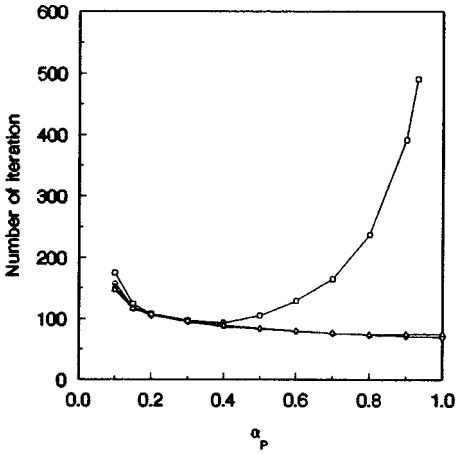

Figure 8. Convergence properties for SIMPLE: $\beta = 60°$, $\alpha_{Ui} = 0.6$.

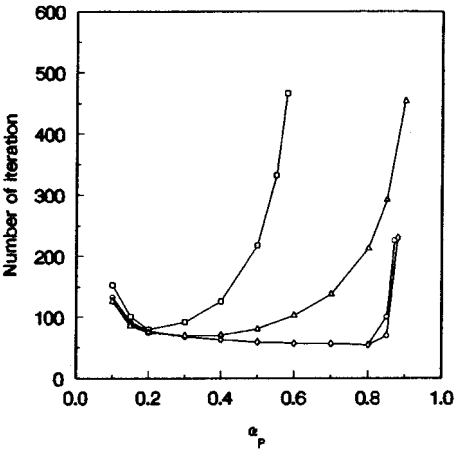

Figure 9. Convergence properties for SIMPLE: $\beta = 60°$, $\alpha_{Ui} = 0.7$.

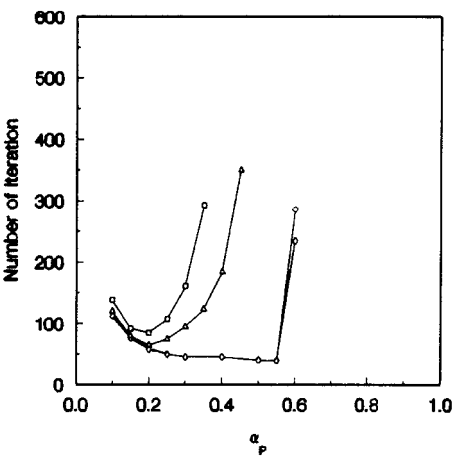

Figure 10. Convergence properties for SIMPLE: $\beta = 60°$, $\alpha_{Ui} = 0.8$.

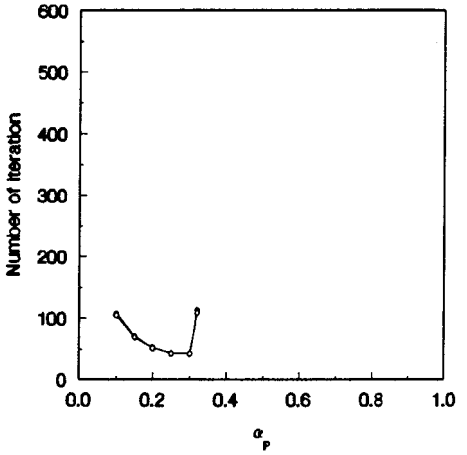

Figure 11. Convergence properties for SIMPLE: $\beta = 60°$, $\alpha_{Ui} = 0.9$

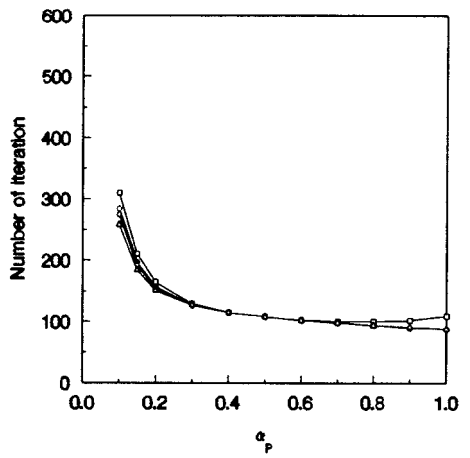

Figure 12. Convergence properties for SIMPLE: $\beta = 45°$, $\alpha_{Ui} = 0.5$.

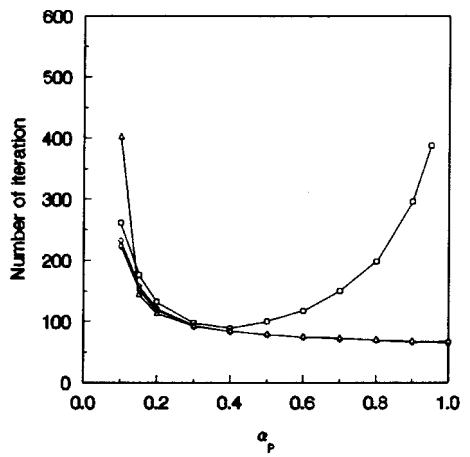

Figure 13. Convergence properties for SIMPLE: $\beta = 45°$, $\alpha_{Ui} = 0.6$.

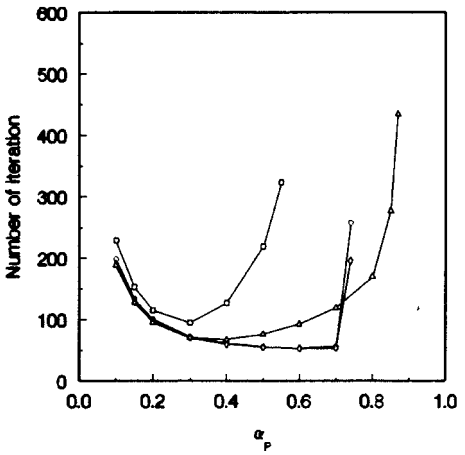

Figure 14. Convergence properties for SIMPLE: $\beta = 45°$, $\alpha_{Ui} = 0.7$.

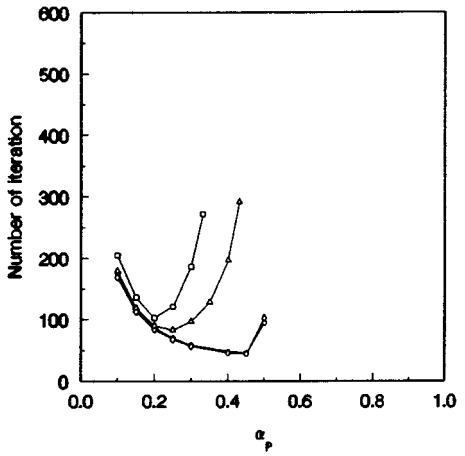

Figure 15. Convergence properties for SIMPLE: $\beta = 45°$, $\alpha_{Ui} = 0.8$.

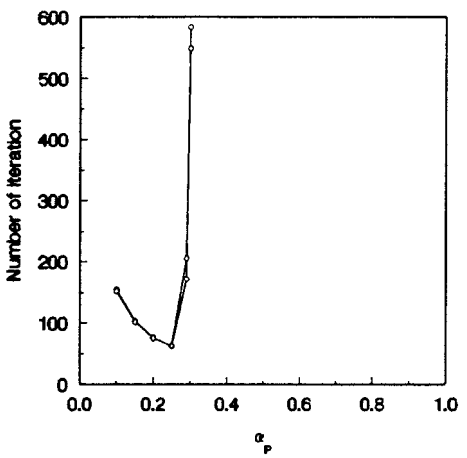

Figure 16. Convergence properties for SIMPLE: $\beta = 45°$, $\alpha_{Ui} = 0.9$.

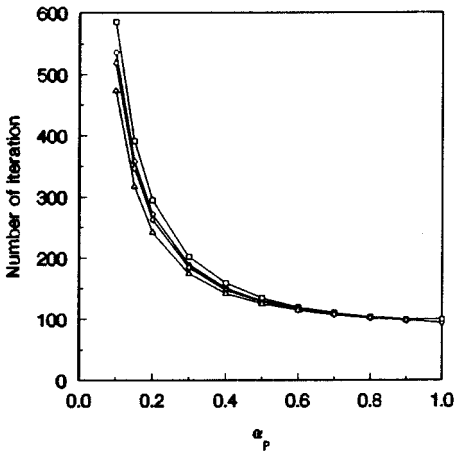

Figure 17. Convergence properties for SIMPLE: $\beta = 30°$, $\alpha_{Ui} = 0.5$.

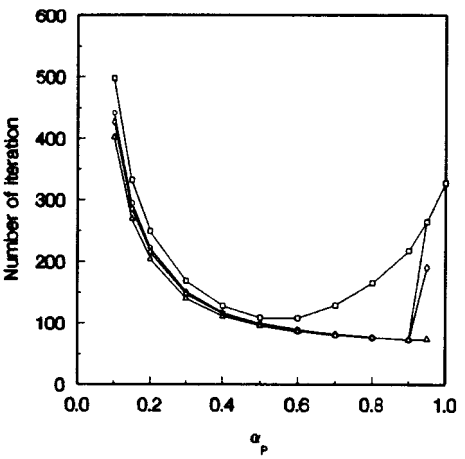

Figure 18. Convergence properties for SIMPLE: $\beta = 30°$, $\alpha_{Ui} = 0.6$.

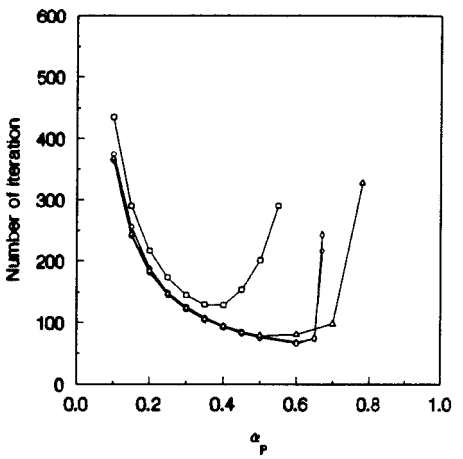

Figure 19. Convergence properties for SIMPLE: $\beta = 30°$, $\alpha_{Ui} = 0.7$.

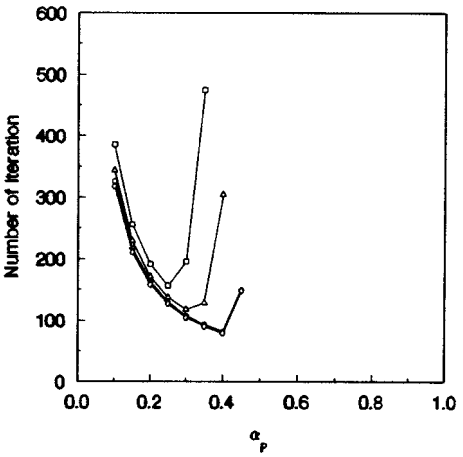

Figure 20. Convergence properties for SIMPLE: $\beta = 30°$, $\alpha_{Ui} = 0.8$.

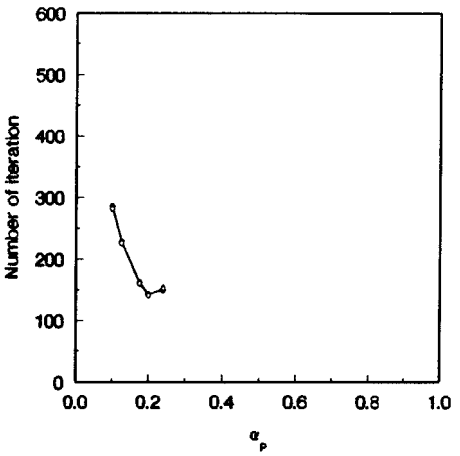

Figure 21. Convergence properties for SIMPLE: $\beta = 30°$, $\alpha_{Ui} = 0.9$.

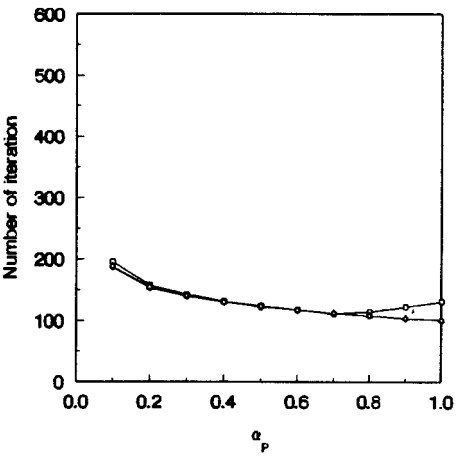

Figure 22. Convergence properties for SIMPLEC: $\beta = 90°$, $\alpha_{Ui} = 0.5$.

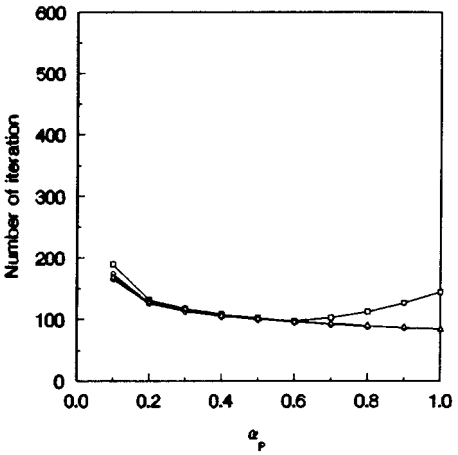

Figure 23. Convergence properties for SIMPLEC: $\beta = 90°$, $\alpha_{Ui} = 0.6$.

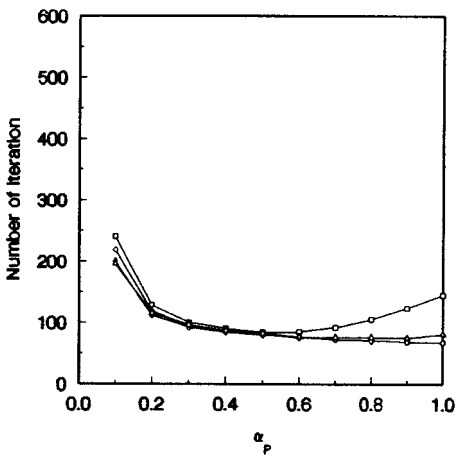

Figure 24. Convergence properties for SIMPLEC: $\beta = 90°$, $\alpha_{Ui} = 0.7$.

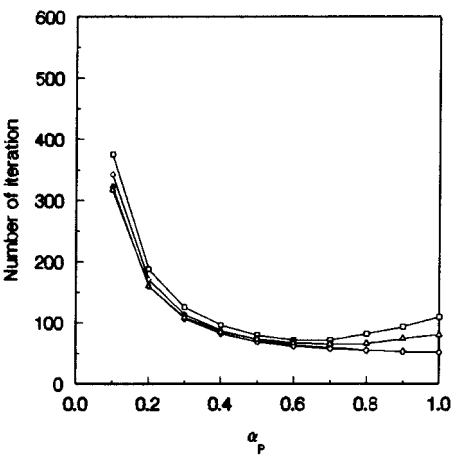

Figure 25. Convergence properties for SIMPLEC: $\beta = 90°$, $\alpha_{Ui} = 0.8$.

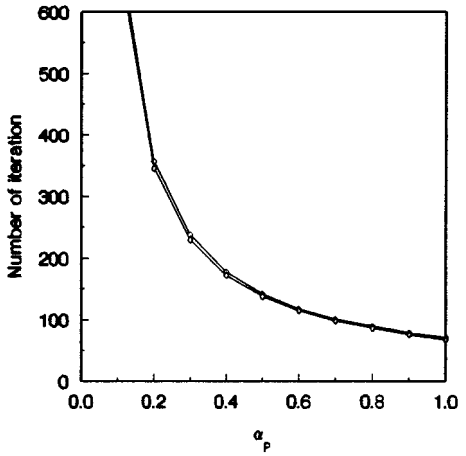

Figure 26. Convergence properties for SIMPLEC: $\beta = 90°$, $\alpha_{Ui} = 0.9$.

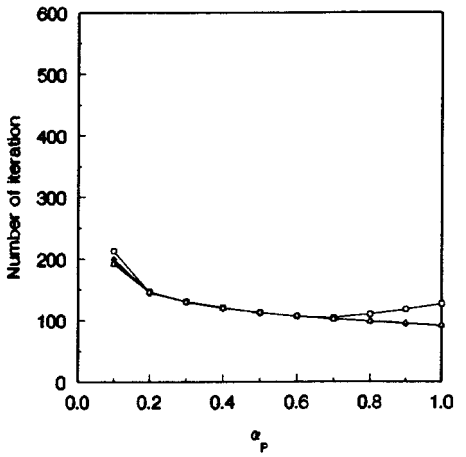

Figure 27. Convergence properties for SIMPLEC: $\beta = 60°$, $\alpha_{Ui} = 0.5$.

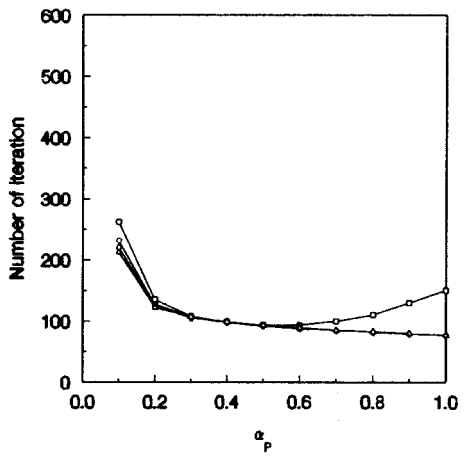

Figure 28. Convergence properties for SIMPLEC: $\beta = 60°$, $\alpha_{Ui} = 0.6$.

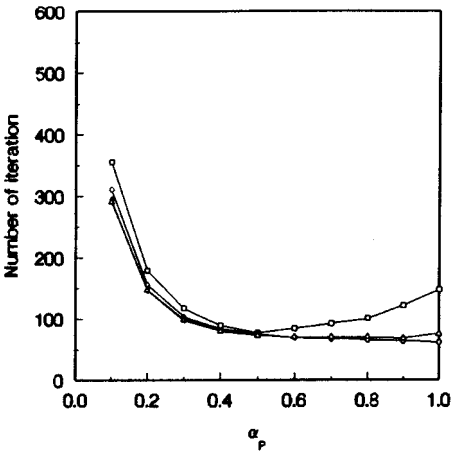

Figure 29. Convergence properties for SIMPLEC: $\beta = 60°$, $\alpha_{Ui} = 0.7$.

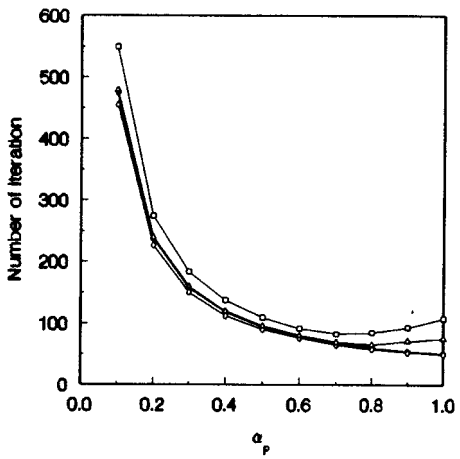

Figure 30. Convergence properties for SIMPLEC: $\beta = 60°$, $\alpha_{Ui} = 0.8$.

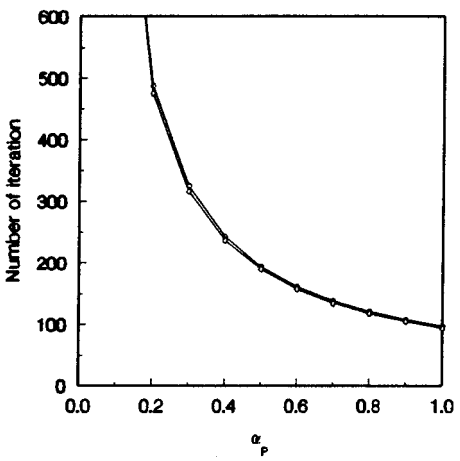

Figure 31. Convergence properties for SIMPLEC: $\beta = 60°$, $\alpha_{Ui} = 0.9$.

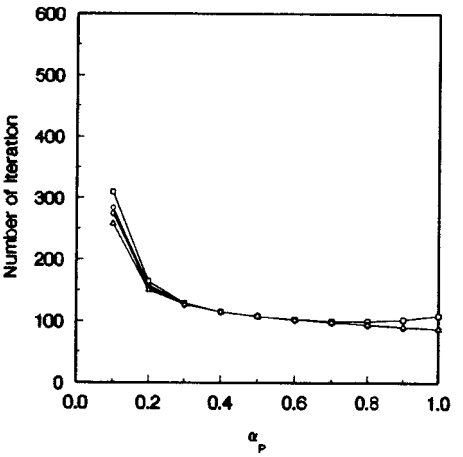

Figure 32. Convergence properties for SIMPLEC: $\beta = 45°$, $\alpha_{Ui} = 0.5$.

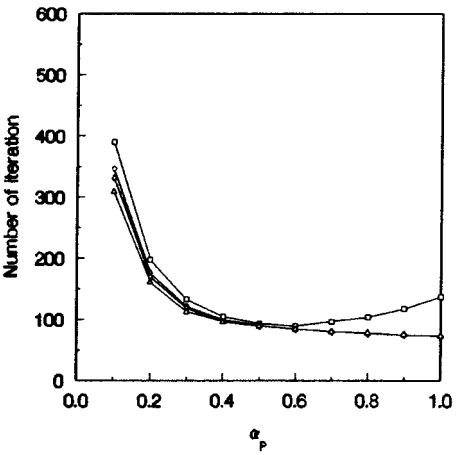

Figure 33. Convergence properties for SIMPLEC: $\beta = 45°$, $\alpha_{Ui} = 0.6$.

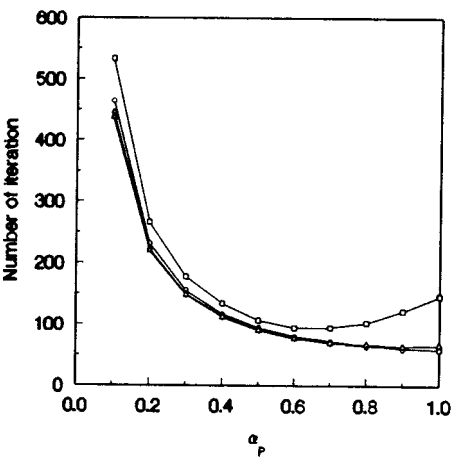

Figure 34. Convergence properties for SIMPLEC: $\beta = 45°$, $\alpha_{Ui} = 0.7$.

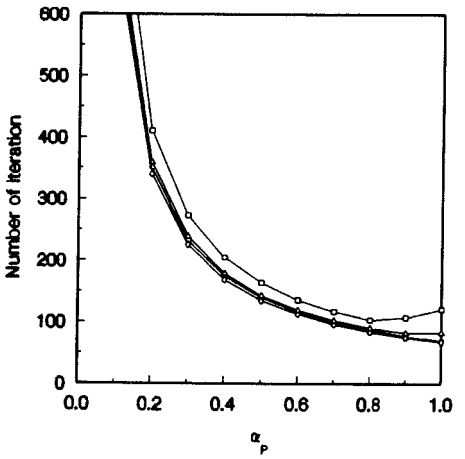

Figure 35. Convergence properties for SIMPLEC: $\beta = 45°$, $\alpha_{Ui} = 0.8$.

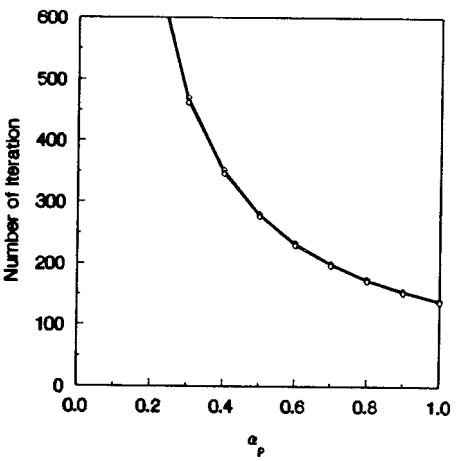

Figure 36. Convergence properties for SIMPLEC: $\beta = 45°$, $\alpha_{Ui} = 0.9$.

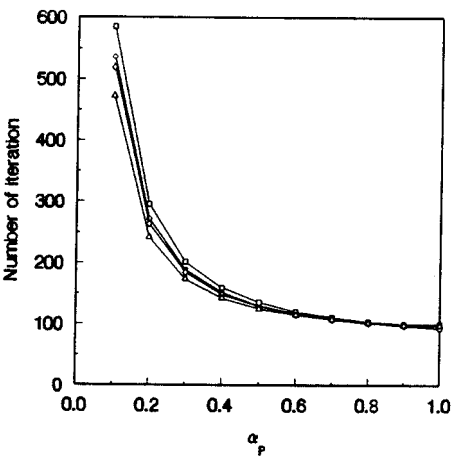

Figure 37. Convergence properties for SIMPLEC: $\beta = 30°$, $\alpha_{Ui} = 0.5$.

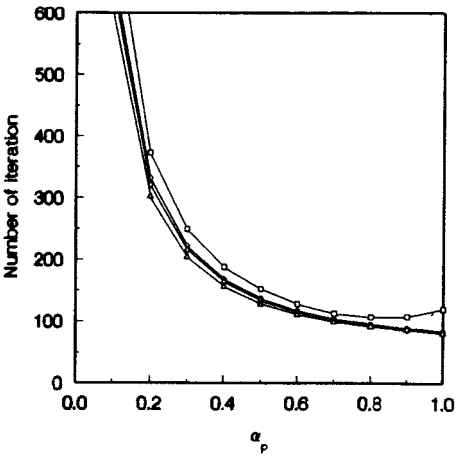

Figure 38. Convergence properties for SIMPLEC: $\beta = 30°$, $\alpha_{Ui} = 0.6$.

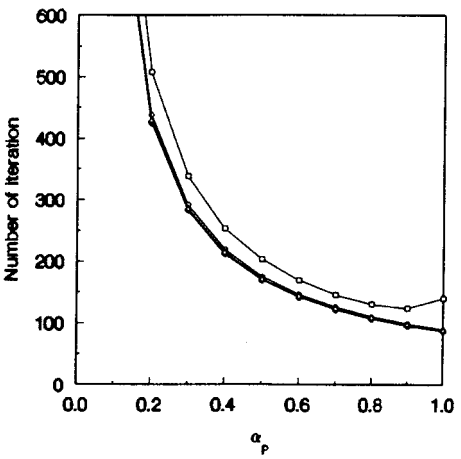

Figure 39. Convergence properties for SIMPLEC: $\beta = 30°$, $\alpha_{Ui} = 0.7$.

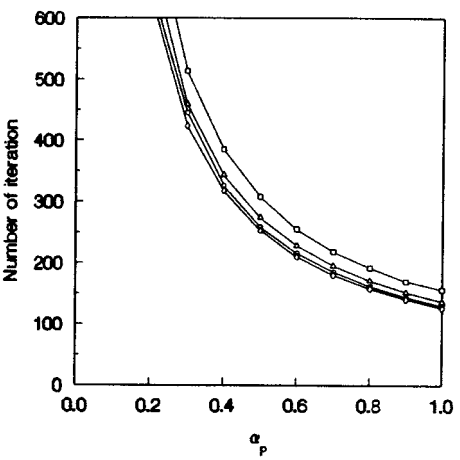

Figure 40. Convergence properties for SIMPLEC: $\beta = 30°$, $\alpha_{Ui} = 0.8$.

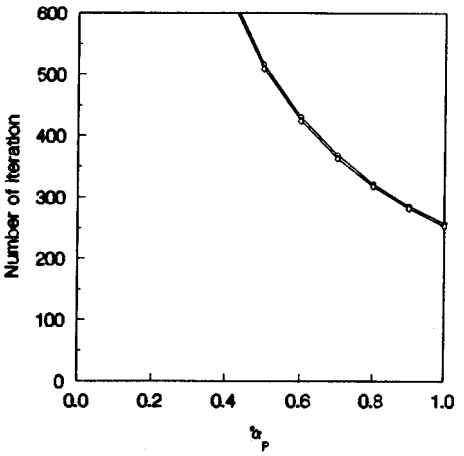

Figure 41. Convergence properties for SIMPLEC: $\beta = 30°$, $\alpha_{Ui} = 0.9$.

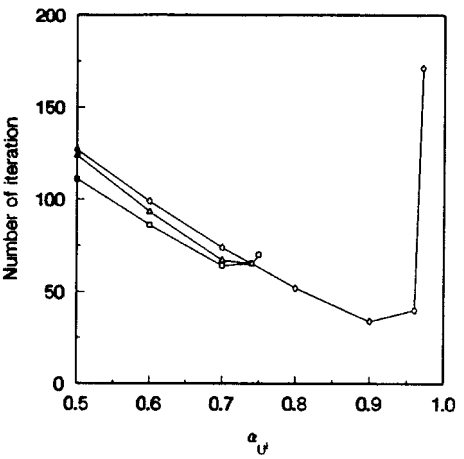

Figure 42. Convergence properties for SIMPLER: $\beta = 90°$.

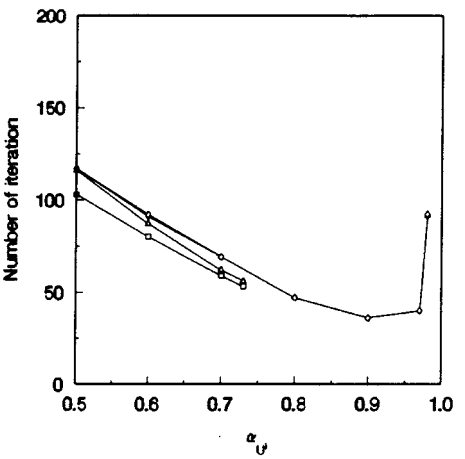

Figure 43. Convergence properties for SIMPLER: $\beta = 60°$.

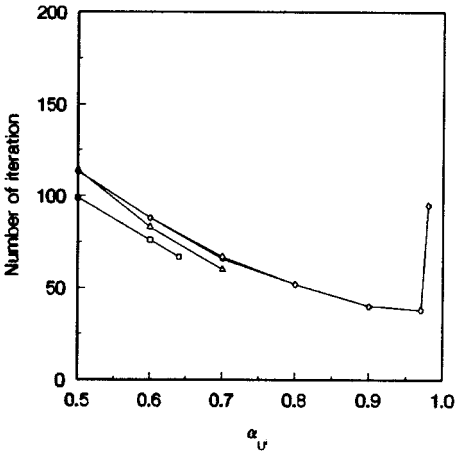

Figure 44. Convergence properties for SIMPLER: $\beta = 45°$.

Figures 22–41 show the number of iterations required for convergence by using the SIMPLE algorithm [3] as a function of the pressure underrelaxation factor, α_p, with the velocity underrelaxation factor, α_{Ui}, as a parameter. Figures 22–26 are for $\beta = 90°$, Figures 27–31 for $\beta = 60°$, Figures 32–36 for $\beta = 45°$, while Figures 37–41 for $\beta = 30°$.

Convergence can always be reached for both practices when α_{Ui} and α_p are very small and cannot be obtained when $\alpha_{Ui} = 1.0$ for both practices. Thus, curves using the SIMPLEC algorithms are formed by connecting 10 points, namely $\alpha_p = 0.1, 0.2, 0.3, \ldots, 1.0$, and the same α_{Ui} values as those used in the case of the SIMPLE algorithm are chosen to be parameter values. Since the convergence cannot be obtained for $\alpha_{Ui} = 0.9$ using practice A, the convergence behaviors obtained using practice A are not plotted in these figures for all the four cases of the cavity flows when $\alpha_{Ui} = 0.9$. There is no limit to the range of α_p values for convergence. That is, the range of α_p values does not become narrower as α_{Ui} increases or β decreases provided that the curve does exist (it does not exist for practice A when $\alpha_{Ui} = 0.9$). For practice B, the optimum α_p value on each curve is always 1.0. But for practice A, this value may not

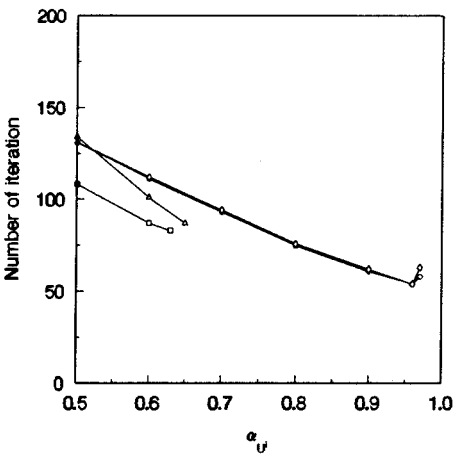

Figure 45. Convergence properties for SIMPLER: $\beta = 30°$.

be 1.0, especially for practice A with α_{U^i}. Still, the number of iterations required for convergence is less for a large β value than that for a small β value. Results obtained from the two cases, with and without α_{U^i}, for practice B are almost identical. As a whole, curves based on practice A without α_{U^i} are closer to those based on practice B than those based on practice A with α_{U^i} if such curves exist. Apparently, practice B behaves better than practice A.

Figures 42–45 show the number of iterations required for convergence by using the SIMPLER algorithm [4] as a function of the velocity underrelaxation factor α_{U^i}. Figure 42 is for $\beta = 90°$, Figure 43 for $\beta = 60°$, Figure 44 for $\beta = 45°$, while Figure 45 for $\beta = 30°$. These figures give some general trends of the convergence characteristics. In the SIMPLER algorithm, no pressure underrelaxation factor is needed to correct the pressure field. The pressure is obtained by solving a Poisson-like equation based on the continuity equation.

Each curve starts at $\alpha_{U^i} = 0.5$. Convergence for both practices when $\alpha_{U^i} < 0.5$ can of course be achieved, but more iterations are needed. The number of iterations decreases as α_{U^i} increases provided α_{U^i} does not exceed a certain value, beyond which a converged solution cannot be obtained. This value for practice A is smaller than that for practice B. Results obtained from the two cases of practice B are almost identical. Apparently, practice B is better than practice A.

Finally, in each solution algorithm (SIMPLE, SIMPLEC and SIMPLER), more iterations reflect more computing time.

3. CONCLUSIONS

In this article, the convergence characteristics of the two-dimensional cavity flows using the two momentum interpolation practices and the three SIMPLE series algorithms (SIMPLE, SIMPLEC and SIMPLER) were presented. In each of the two practices, two situations, i.e. with and without velocity underrelaxation factors in the momentum interpolation formulations, are considered. The angle between the side wall of the cavity and the horizontal line, β, was set to be 90, 60, 45 and 30°. The velocity underrelaxation factor, α_{U^i} was set to be 0.5, 0.6, 0.7, 0.8 and 0.9.

For both practices, no converged solution can be reached using the three SIMPLE series algorithms when $\alpha_{U^i} = 1.0$. $\alpha_{U^i} = 0.9$ is too high for the convergence using practice A to be achieved. For practice B, $\alpha_{U^i} = 0.9$ leads to converged solutions. For the results obtained using the SIMPLE algorithm, a range of the α_p values for convergence exists when α_{U^i} is high for both practices. The range α_p values gets narrower as β decreases or α_{U^i} increases. For the results obtained using the SIMPLEC algorithm, there is no restrictions on the α_p values, even if the grid skewness is highly non-orthogonal ($\beta = 30°$) and a high α_{U^i} value ($\alpha_{U^i} = 0.8$ for practice A and $\alpha_{U^i} = 0.9$ for practice B) is used provided the convergence can be obtained. This means that the full pressure-correction equation or any its modified forms are not necessary in order to obtain a wider range of α_p values, and the simplified pressure-correction equation is capable of achieving this goal. For the results obtained using the SIMPLER algorithm, the critical α_{U^i} value for practice A, beyond which no convergence can be obtained, is smaller than that for practice B. Little difference between the curves with and without α_{U^i} value using practice B can be observed. This means that whether the velocity underrelaxation factor appears in the momentum interpolation formulation for practice B does not affect the convergence rate. Comparatively, practice A without α_{U^i} is superior to practice A with α_{U^i}. Practice B gives better convergence behaviors than practice A.

APPENDIX A. NOMENCLATURE

L cavity length
Re Reynolds number
u_L lid velocity
α_p pressure underrelaxation
α_{U^i} velocity underrelaxation factor
β angle between the cavity side wall and the horizontal line
μ dynamic viscosity
ρ density

REFERENCES

1. H. Xu and C. Zhang, 'Study of the effect of the non-orthogonality for non-staggered grids—the theory', *Int. J. Numer. Methods Fluids*, **28**, 1265–1280 (1998).
2. S.V. Patankar and D.B. Spalding, 'A calculation procedure for heat, mass and momentum transfer in three-dimensional parabolic flows', *Int. J. Heat Mass Transf.*, **15**, 1787–1806 (1972).
3. S.V. Patankar, *Numerical Heat Transfer and Fluid Flow*, Hemisphere, Washington, DC, 1980.
4. J.P. Van Doormaal and G.D. Raithby, 'Enhancements of the SIMPLE method for predicting incompressible fluid flows', *Numer. Heat Transf.*, **7**, 147–163 (1984).
5. M. Peric, 'Analysis of pressure–velocity coupling on non-orthogonal grids', *Numer Heat Transf. B.*, **17**, 63–82 (1990).
6. M.J. Cho and M.K. Chung, 'New treatment of non-orthogonal terms in the pressure-correction equation', *Numer. Heat Transf. B*, **26**, 133–145 (1994).

